WPJET1-PR(18) 21488

CG Silva et al.

GAM evolution in L-mode approaching the L-H transition on JET

Preprint of Paper to be submitted for publication in
Plasma Physics and Controlled Fusion

This work has been carried out within the framework of the EUROfusion Consortium and has received funding from the Euratom research and training programme 2014-2018 under grant agreement No 633053. The views and opinions expressed herein do not necessarily reflect those of the European Commission.

GAM evolution in L-mode approaching the L-H transition on JET

C. Silva[1], J. C. Hillesheim[2], L. Gil[1], C. Hidalgo[3], C.F. Maggi[2], L. Meneses[1], E.R. Solano[3], and JET Contributors*

EUROfusion Consortium, JET, Culham Science Centre, Abingdon, OX14 3DB, UK

[1]Instituto de Plasmas e Fusão Nuclear, Instituto Superior Técnico, Universidade Lisboa, PT

[2]CCFE, Culham Science Centre, Abingdon, OX14 3DB, UK

[3]Laboratorio Nacional de Fusión, CIEMAT, 28040 Madrid, Spain

** See the author list of "X. Litaudon et al 2017 Nucl. Fusion 57 102001"*

Abstract

Geodesic acoustic modes (GAMs) may generate strong oscillations in the radial electric field and therefore are considered as a possible trigger mechanism for the L–H transition. This contribution focuses on the characterization of GAMs in JET plasmas when approaching the L-H transition aiming at understanding their possible role in triggering the transition. GAM and turbulence characteristics are measured at the plasma edge using Doppler backscattering for different plasma current and line-averaged densities. The radial location of the GAM often moves further inside when NBI is applied possibly as a response to changes in the turbulence drive. GAMs are found to have modest amplitude at the transition except for high density discharges where GAMs are stronger, suggesting that the GAM is not responsible for facilitating the transition as the L-H power threshold also increases with density in the high density branch of the L-H transition. Our results suggest that the GAM alone does not play a leading role for causing the L-H transition at JET.

Introduction

Geodesic acoustic modes (GAMs) are oscillating zonal flows (ZFs) capable of regulating turbulence and the associated transport [e.g. 1, 2]. This was experimentally corroborated by findings in different devices demonstrating the importance of both the oscillating and mean flow shear and their interaction [e.g. 3-5]. The shearing due to ZFs is thought to dominate in regimes when the mean shear flow is modest as before and during the L-H transition [3-10].

Understanding the interaction between ZFs and turbulence is therefore crucial to control plasma confinement.

ZFs may generate strong oscillations in the radial electric field which is widely recognized to play an important role in the transition to improved confinement regimes [e.g. 11-12]. Consequently, the importance of ZFs as a possible trigger for the L–H transition has been investigated in different devices [3, 6-10]. For ASDEX Upgrade low plasma density discharges [3], limit cycle oscillations (LCOs) are formed in an intermediate phase (I-phase) before the transition to H-mode with competing turbulence drive and enhanced flow shearing, where the GAM flow shearing plays an important role. A strong interaction between GAMs and LCOs was also found on HL-2A [7]. However, the GAM intensity decreased at the onset of LCOs, indicating an energy transfer from GAMs to LCOs and suggesting that the GAM can assist the transition from L-mode to the I-phase but does not play a significant role in the I-H transition. In an earlier work at HL-2A [8], the energy transfer from turbulence into GAMs and the GAM amplitudes was reported to increase as the heating power was increased, peak and then decrease, while the energy transfer into the low-frequency ZFs (LFZFs) increased monotonically with heating power, suggesting that LFZFs play an important role in the L-H transition. Similarly, on DIII-D [9] the turbulence poloidal flow spectrum was reported to evolve from GAM dominated at lower power to LFZF dominated near the L–H transition. At lower electron density, a clear increase of the LFZF was observed prior to the L–H transition, which was not evident at higher density. The possibility of L–H transition initiation by GAMs was also investigated on TUMAN-3M [10], with the L–H transition always found to be preceded by GAM-like oscillations at low density.

In summary, while on ASDEX Upgrade the sheared flow below the L-H threshold is dominated by GAMs, on devices such as DIII-D and HL-2A GAMs do not appear to be important on the way to H-mode. The reported results reveal that no clear picture exists on the relevance of GAMs in the turbulence collapse required for the formation of steep pressure gradients at the transition. The GAM relevance for the L-H transition may be related with the parameter space for the GAM existence that is related to their driving and damping mechanisms which varies between experimental devices.

This contribution focuses on the characterization of GAMs in JET plasmas when approaching the L-H transition aiming at understanding their possible role in triggering the transition. We build on previous JET work [13, 14] based on a Doppler backscattering dataset of GAM measurements aiming at understanding the dependence of the GAM amplitude on the plasma parameters, using as main experimental knobs the plasma current and the discharge density.

Here, the work is expanded to include the effect of the heating power on the GAM characteristics, taking advantage of the scaling of the GAM amplitude previously established [14].

Description of the experiment

Doppler backscattering (DBS) is a microwave diagnostic for density fluctuation measurements that measures the radially localized propagation velocity and fluctuation level of intermediate wavenumber turbulent structures. The JET correlation reflectometer [15] consists of two X-mode fast frequency hopping (≤ 60 μs) channels launched from the LFS midplane with probing frequencies variable in the range 75 – 110 GHz (W-band). Each channel can be pre-programmed with a specified launch frequency pattern, which is repeated continuously throughout the discharge, allowing a radial scan of the measurement location. This diagnostic has been used previously at JET to characterize GAMs [13], where a detailed description of the diagnostic together with an explanation of the GAM analysis method can be found. As described in [13], results presented here correspond to the peak-to-peak amplitude of the measured perpendicular velocity at the GAM frequency with an associated uncertainty in the order of 0.1 km/s.

For the data presented here, the reflectometer channel 1 (master) was typically set to a 14 point frequency sweep (from 73.46 to 96.47 GHz), while channel 2 (slave) had an 11 point frequency sweep of 2 ms duration around each master frequency with the full frequency sweep taking 308 ms. Most of the analysis was performed with the DBS master signals. The use of the slave signal may seem advantageous as it allows a finer radial resolution of the measurements (there are 11 slave frequency steps within each master one). It is however important to note that the intermittency in the GAM amplitude has to be taken into account when using the slave signals. As shown in [13], the GAM amplitude is highly intermittent in a time scale of a few ms. As the duration of the slave frequency step is only 2 ms, the GAM intermittency leads to a larger scatter in the estimate of the GAM amplitude. Analysis performed with the slave signal provides therefore a higher spatial resolution at a cost of a reduced statistics and it is only used here to estimate the density fluctuation level.

GAM measurements have been obtained in plasma current ($2.2 < I_p < 3.2$ MA) and line-averaged density ($1.6 < \bar{n} < 3.6\times10^{19}$ m^{-3}) scans designed to determine the underlying mechanisms that influence the L–H power threshold scaling [16]. The L–H transitions were induced by slowly increasing the neutral beam injection (NBI) heating power in corner

configuration discharges (plasmas with both divertor strike-points in the corner between the horizontal and vertical targets close to the pump throat). Discharges at 2.5 MA/3.0 T in vertical target configuration (plasmas with both divertor strike-points in the vertical targets) where the NBI power was scanned in steps from 1 to 9 MW in both hydrogen and deuterium while keeping the plasma density constant to $\bar{n} \sim 3.0\times10^{19}$ m^{-3} were also analyzed [17].

Previous studies based on the ohmic phase of the discharges in the dataset demonstrated that parameters such as $\bar{n}$ and I_p have a strong effect on the GAM amplitude [13, 14]. By assessing the importance of critical parameters such as safety factor and collisionality, experimental evidence was found for the different mechanisms determining the GAM amplitude: turbulence drive, collisional and collisionless damping. Evidence for collisional damping was only found at low I_p, high density discharges. For the remaining dataset, the GAM amplitude was well described by a balance between turbulence drive and collisionless damping [14].

Heating power dependence of the GAM amplitude

GAMs have been studied along the power ramp used to induce the L–H transition, taking advantage of the unique JET dataset. The temporal evolution of the mean perpendicular velocity, normalized density fluctuation level and GAM amplitude for different probing frequencies is presented in figure 1 for a typical discharge with an L-H transition (#90484, I_p = 2.5 MA, B_T = 3 T, $\bar{n} = 3.2 \times 10^{19}$ m^{-3}) with the respective radial profiles shown in figure 2 for selected periods with different NBI power. As NBI heating is applied, the equilibrium flow profile is generally observed to move upward but then exhibits a modest variation with the NBI power up to the transition. No significant increase of the equilibrium flow shear is observed near the L–H transition. A modest equilibrium flow is typically observed at the edge plasma for corner configuration discharges, contrary to the observed for instance for the vertical target configuration. For this latter case, a clear increase of the edge shear flow with heating power is seen associated with a reduction of the density fluctuations levels. For the discharges analyzed here, the transition occurs directly from L- to H-mode with no LCO phase, although a short M-mode [18] phase is sometimes observed after the L-H transition that shares some common features with the I-phase. GAM are clearly visible during the ohmic period but shortly after the NBI power is applied, the GAM amplitude is reduced decreasing further as the L-H transition is approached. Although the GAM amplitude is sometimes observed to first increase with heating power, it is in general reduced before the L-H transition. The GAM amplitude near the transition is typically larger for high density discharges in agreement with previous observations revealing that the GAM amplitude tends to increase with density [13, 14]. The

large turbulence amplitude associated with the high density discharges may provide a stronger drive for GAMs.

GAMs have either modest amplitude at the transition or are below detectable limits for the technique applied here. The cause of this decrease in the GAM amplitude may be related with the reduction of the turbulence levels in the region where GAMs are observed (edge density gradient region near the pedestal top, see figures 1 and 2) when the NBI power is applied due to changes in the plasma rotation profile induced by the NBI torque. However, changes in the density fluctuation levels in this region are modest (~10%), with the ohmic values recovered later on along the heating power ramp. As the collisional damping rate (proportional to the ion collision rate) is also expected be reduced along the power ramp, it is unclear why GAMs are not observed at a later L-mode phase of the discharge and why they are reduced before L-H the transition.

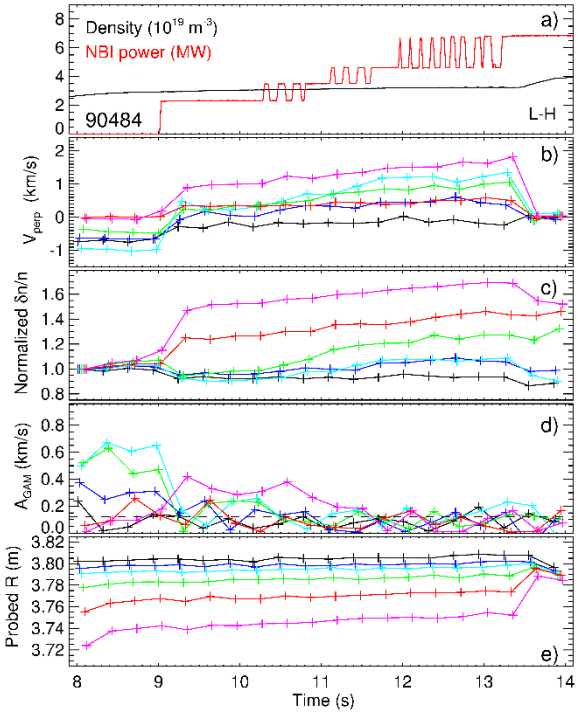

Figure 1: Temporal evolution of density and heating power (a), mean perpendicular velocity (b), density fluctuation level normalised to the value at t ~ 8 s (c) and GAM amplitude with the minimum detectable GAM amplitude indicated by the dashed horizontal line (d) for discharge #90484 for different probing frequencies with the respective probing location shown in (e). The time of the L-H transition is indicated by the vertical line.

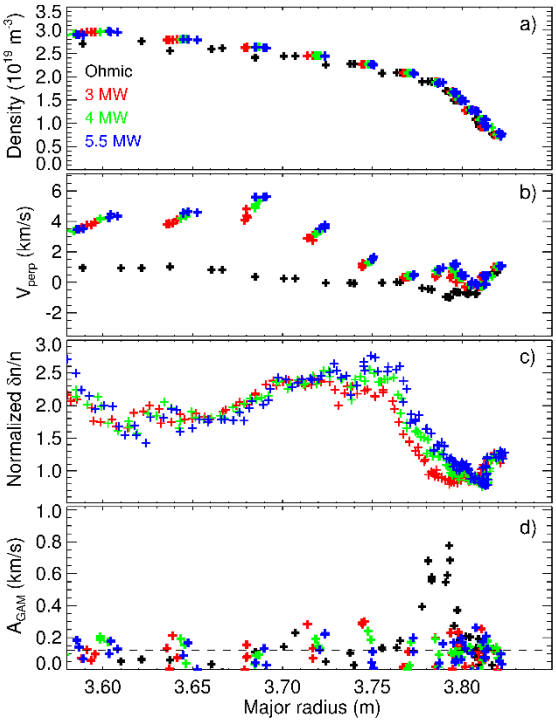

Figure 2: Radial profiles of density (a), mean perpendicular velocity (b), density fluctuation level normalized to the profile in the ohmic phase (c) and GAM amplitude with the minimum detectable GAM amplitude indicated by the dashed horizontal line (d) for discharge #90484 for different NBI power levels. The separatrix is at 3.81 (±0.01) m. The L-H transition occurs at P_{NBI} ~6.8 MW.

GAM radial location

Figure 3 displays the radial profiles of the mean perpendicular velocity, normalized density fluctuation level and GAM amplitude for discharge #90492 (I_p = 2.5 MA, B_T = 3 T, $\bar{n}$ = 3.6 × 10^{19} m^{-3}) with a higher line-averaged density compared to the discharge shown in figures 1 and 2. In this case, the GAM survives up to the L-H transition. As NBI heating is applied, the density fluctuation levels decreases slightly (~10%) in the steep gradient region, increasing significantly inside the pedestal top (factor of ~2). The equilibrium flow profile is clearly observed to move upward when the NBI power is applied but then exhibits a modest variation with the NBI power up to the transition.

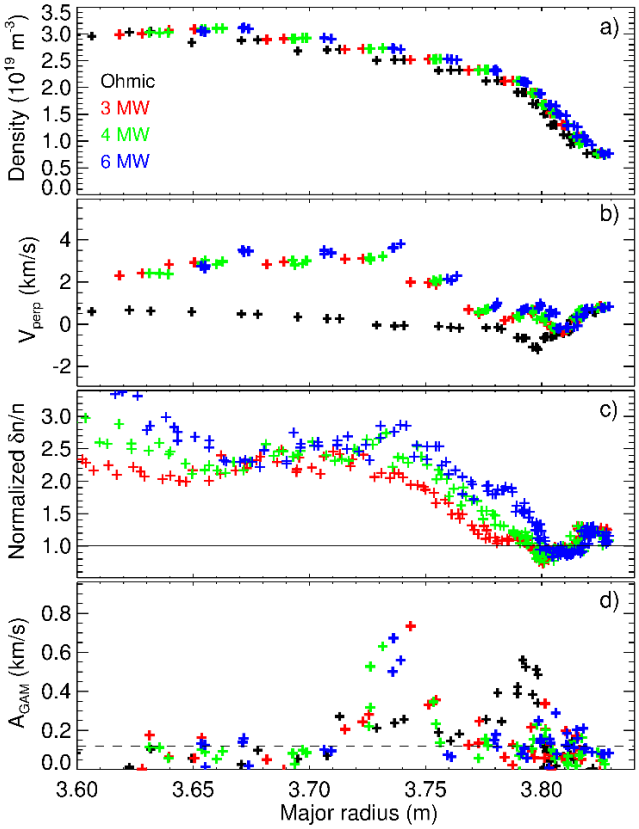

Figure 3: Radial profiles of density (a), mean perpendicular velocity (b), normalized density fluctuation level (c) and GAM amplitude (d) for discharge #90492 for different NBI power levels. The separatrix is at 3.81 (±0.01) m. The L-H transition occurs at P_{NBI} ~7.5 MW.

During the ohmic phase, GAMs are generally most intense in the edge density gradient region near the pedestal top. As the heating power is ramped up, the GAM amplitude decreases near the pedestal top in the region where the fluctuations levels are reduced, appearing further inside in a region where density fluctuations increase. As the diagnostic is not absolutely calibrated, we can only compare variations with respect to reference measurements and therefore cannot conclude about the absolute fluctuations level at the different radial locations. Apart from

changes in the turbulent drive the balance between the collisional and collisionless damping rates should also play a role in the radial variation of the GAM location, with damping rates having opposite trends with radius: collisional damping ($\propto$ ion collision rate) increases with radius, contrary to the collisionless damping rate ($\propto exp[-q^2]$, where q is the safety factor). It is interesting to note that the GAM existence region does not appear to be continuous, moving from ~2 cm to ~7 cm inside the separarix.

Figure 4 shows the temporal evolution of the line-averaged density, heating power and reflectometry probing frequency, together with the spectrogram of the Doppler shift. As illustrated, the frequency spectrum is sharply peaked at ~7 kHz during the ohmic phase. Shortly after the NBI power is applied the dominant GAM frequency shifts to ~11 kHz. Also shown in figure 4 (solid lines) is the calculated GAM frequency using the local temperature given by different ECE channels revealing that the evolution of main GAM frequency is not consistent with that of the local temperature at a single position but rather with the local frequency at two distinct radial locations.

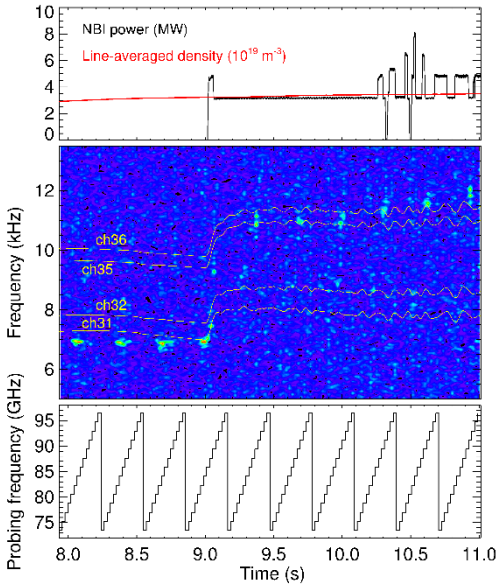

Figure 4: Temporal evolution of the density, heating power, spectrogram of the reflectometry Doppler shift and probing frequency for discharge #90492. The solid lines overlayed in the spectrogram indicate the GAM frequency estimated using the local electron temperature given by different ECE channels.

Coexisting GAMs of different frequencies have been observed with Langmuir probes in the edge plasma of HL-2A tokamak in low density Ohmic discharges [19] and with DBS on DIII-D [20]. The GAM on HL-2A was found to propagate both inward and outward with its frequency remaining the same during the process. The GAM structure at JET seems to be different. GAMs with different frequencies do not appear to coexist at the same radial locations

contrary to HL-2A and DIII-D observations. The existence region of the GAMs with different frequency is separated by about 5 cm having a radial extension limited to about 2 cm. This suggests that GAMs are strongly damped with a decay length in the order of cm, only existing in the region where they are generated. As the collisionality increases with radius the GAM outward propagation may be limited by collisional damping.

Isotope effect

The impact of the isotope mass on the GAM amplitude has also been investigated by comparing hydrogen and deuterium plasmas. DBS data available from L-mode pulses obtained in recent JET experiments with NBI heating at 2.5 MA/3.0 T. The NBI power was scanned from 1 to 9 MW in both hydrogen and deuterium while keeping the plasma density constant to $\bar{n} \sim 3.0\times10^{19}$ m^{-3} (obtained with feedback control on the injected gas) [17]. The heating power available in the experiment was enough to reach H-mode in deuterium at B_T = 3 T but not in hydrogen plasmas where the required power is expected to be larger by a factor around two [17].

The dependence of the GAM amplitude on the NBI heating power for hydrogen and deuterium plasmas is shown in figure 5a. Results indicate that the GAM amplitude in the ohmic phase of the discharge is larger for deuterium plasmas by about 20% in agreement with previous findings at JET [13]. However, above a certain heating power (P_{NBI} ~4 MW), the GAM amplitude increases in hydrogen and decreases in deuterium plasmas. This may be related with the higher turbulence levels in hydrogen than deuterium plasmas [17]. At a power level just below the power threshold in deuterium, GAMs are significantly larger for hydrogen plasmas. However, as the L-H transition was not reached for hydrogen plasmas may be the case that also in hydrogen the GAM amplitude is reduced before the L-H transition. In fact, when plotting the results as a function of the NBI power normalized to the power threshold (see figure 5b), the GAM amplitude exhibits a similar trend in both H and D plasmas. Therefore, the possibility that the GAM amplitude is reduced before the transition in H plasmas cannot be discarded. For the normalization of the NBI power it was assumed that the ratio of the power threshold in H to that measured in D at 3 T is 2.4, corresponding to the ratio observed at 1.8 T for the same density [17].

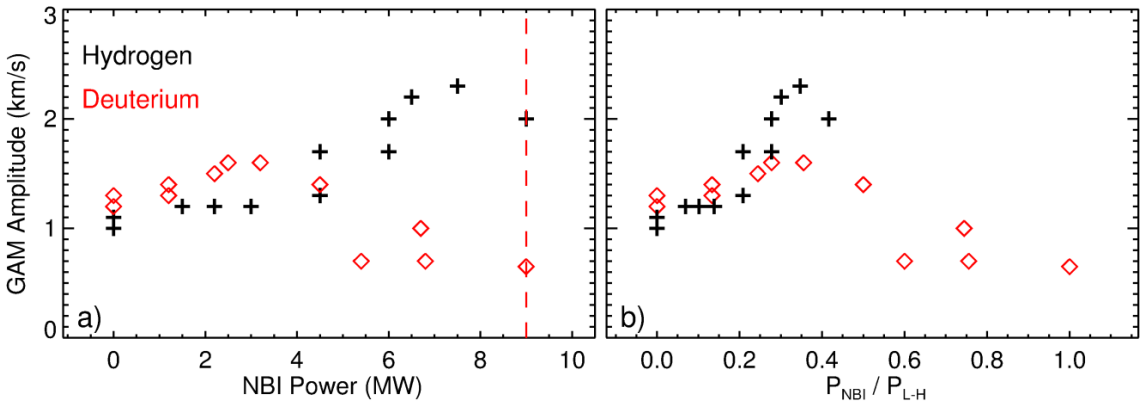

Figure 5: Dependence of the GAM amplitude on the NBI heating power (a) and NBI heating power normalized to the power threshold (b)for hydrogen and deuterium plasmas at I_p = 2.5 MA, B_T = 3.0 T and $\bar{n}$ ~3.0×10^{19} m^{-3}. The power required for the L-H transition in deuterium plasmas is indicated by the vertical line.

Discussion and summary

In this work, the GAM and turbulence characteristics are measured at the plasma edge for different plasma current and line-averaged densities to investigate how they impact on the L–H transition. GAMs are found to have modest amplitude at the transition except for high density discharges. The large turbulence amplitude associated with the high density discharges may provide a stronger drive for GAMs. These observations suggest that the GAM is not responsible for facilitating the transition as the L-H power threshold also increases with density in the high density branch of the L-H transition. In addition, the dependence of the GAM amplitude on plasma current is also not consistent with that of the L-H power threshold. While the L-H power threshold was found to be roughly independent of the plasma current in the high density branch of the L-H transition [16], GAMs are suppressed at high plasma current due to collisionless damping [14]. Furthermore, in the low density branch of the L-H transition, both the GAM amplitude and the L-H power threshold increase with plasma current [21]. The dependence of the GAM amplitude on plasma current and density is therefore not qualitatively consistent with the L-H power threshold scaling relations.

Our results suggest that the GAM alone should not play a leading role for causing the L-H transition at JET. In spite of being routinely observed at JET at low heating power, sometimes associated with large flow oscillations (in the order of 2 km/s), no clear indication of L–H transitions triggered by the GAM was found. In JET experiments the L–H transitions are rarely accompanied by GAMs with amplitude significantly larger than the detection threshold.

The causes for the decrease of the GAM amplitude before L-H the transition are however unclear. Density fluctuation levels are slightly reduced in the region where GAMs are observed when the NBI power is applied but the ohmic values are recovered later on along the heating power ramp indicating that the turbulence drive is not reduced. The collisional damping rate (proportional to the ion collision rate) is expected be reduced along the power ramp while the collisionless damping rate (proportional to $exp[-q^2]$) is not changed. It should be noted however that recent estimates for the collisionless damping rate including finite orbit drift width effects [22] predict that the GAM damping rate depends strongly on the normalized radial wavenumber $k_r\rho_i$, where k_r is the GAM radial wavenumber and ρ_i the ion Larmor radius. Assuming that k_r does not depend on the heating power (no systematic study was performed at JET on the k_r dependence on the plasma parameters) the damping rate will be influenced mainly by the temperature evolution [14]. It is expected therefore that the collisonless damping rate including finite orbit drift width effects will increase along the heating power ramp, possibly justifying the decrease of the GAM amplitude when approaching the L-H transition.

Interesting results are also reported with respect to changes in the GAM radial location possibly as a response to modifications in the turbulence drive. GAMs are often supressed near the pedestal top when NBI is applied, appearing further inside in the flat gradient region where the density fluctuation level increases. However, GAMs at the two radial locations do not appear to coexist. The GAM existence region is limited to about 2 cm, suggesting a strong damping with a decay length in the order of cm.

Different reports have presented experimental evidence that the turbulence poloidal flow spectrum evolves from GAM dominant at lower power to low-frequency ZF dominant near the L–H transition associated with an increase of the effective shearing rate [8, 9]. Although no significant change in the mean perpendicular velocity seems to occur preceding the transition, the temporal resolution of the measurements for each probing frequency is only ~300 ms for the diagnostic settings used in this experiment and therefore the fast dynamics near the transition cannot be studied. As LFZFs have been identified at JET [23], a systematic study of the evolution of LFZFs and GAMs as the L-H transition is approached should be performed with a suitable temporal resolution to assess a possible competition between LFZFs and GAMs for the transfer of turbulent energy.

Acknowledgements
This work has been carried out within the framework of the EUROfusion Consortium and has received funding from the Euratom research and training programme 2014-2018 under grant agreement No 633053. IST activities also received financial support from "Fundação para Ciência e Tecnologia" through project UID/FIS/50010/2013. The views and opinions expressed herein do not necessarily reflect those of the European Commission.

References

[1] P.H. Diamond, S.-I. Itoh, K. Itoh and T.S. Hahm, Plasma Phys. Control. Fusion 47, R35 (2005)
[2] A. Fujisawa, Nucl. Fusion 49, 013001 (2009)
[3] G. D. Conway, C. Angioni, F. Ryter, P. Sauter, J. Vicente, Phys. Rev. Lett. 106, 065001 (2011)
[4] T. Estrada et al, Nucl. Fusion 51 032001 (2011)
[5] C. Silva et al, Nucl. Fusion 58 026017 (2018)
[6] G.S. Xu et al, Phys. Rev. Lett. 107 125001 (2011)
[7] M. Xu et al, Phys. Rev. Lett. 108 245001 (2012)
[8] A. S. Liang et al, Phys. Plasmas 25 022501 (2018)
[9] Z. Yan et al, Nucl. Fusion, 53 113038 (2013)
[10] L. G. Askinazi et al., Plasma Phys. Control. Fusion 59 014037 (2017)
[11] C. P. Ritz et al, Phys. Rev. Lett. 65 2543 (1990)
[12] R. Moyer et al, Phys. Plasmas 2 2397 (1995)
[13] C. Silva et al, Nucl. Fusion 56 106026 (2016)
[14] C. Silva et al, Plasma Phys. Control. Fusion 60 (2018) 085006
[15] J.C. Hillesheim et al., Proc. 12th Inter. Reflectometry Workshop - IRW12, Juelich, Germany (2015)
[16] "Role of stationary zonal flows and momentum transport for L-H transitions in JET", J.C. Hillesheim et al, 26th Fusion Energy Conference, 2016
[17] C. Maggi et al, Plasma Phys. Control. Fusion 60 014045 (2018)
[18] E.R. Solano et al, Nucl. Fusion 57 022021 (2017)
[19] D.F. Kong et al, Nucl. Fusion 57 044003 (2017)
[20] J.C. Hillesheim et al, Phys. Plasmas 19 022301 (2012)
[21] "Overview and Interpretation of L-H Threshold Experiments on JET with the ITER-like Wall", E. Delabie et al, 25th Fusion Energy Conference, 2014
[22] Z. Gao, Plasma Science and Technology 13, 15 (2011)
[23] J.C. Hillesheim et al, Phys. Rev. Lett. 116, 065002 (2016)